International Journal of Food Science +Technology

Institute of Food Science +Technology ifst

International Journal of Food Science and Technology 2023

Original article

Cerrado and Pantanal fruit flours affect gut microbiota composition in healthy and post-COVID-19 individuals: an *in vitro* pilot fermentation study

Carolina Saori Ishii Mauro,[1] Maryame Kadiri Hassani,[2] Monica Barone,[3] Maria Teresa Esposito,[2] Yolanda Calle,[2] Volker Behrends,[2] Sandra Garcia,[1] Patrizia Brigidi,[3] Silvia Turroni[4]* & Adele Costabile[2]

1 Department of Food Science and Technology, State University of Londrina, Londrina 86057-970, Brazil
2 School of Life and Health Sciences, University of Roehampton, London SW15 4JD, UK
3 Microbiomics Unit, Department of Medical and Surgical Sciences, University of Bologna, Bologna 40138, Italy
4 Unit of Microbiome Science and Biotechnology, Department of Pharmacy and Biotechnology, University of Bologna, Bologna 40126, Italy

(Received 2 November 2022; Accepted in revised form 21 December 2022)

Summary Cerrado and Pantanal plants can provide fruits with high nutritional value and antioxidants. This study aims to evaluate four fruit flours (from jatobá pulp, cumbaru almond, bocaiuva pulp and bocaiuva almond) and their effects on the gut microbiota in healthy (HD) and post-COVID-19 individuals (PC). An *in vitro* batch system was carried out, the microbiota was analysed by 16S rRNA amplicon sequencing and the short-chain fatty acids ratio was determined. Furthermore, the effect of jatobá pulp flour oil (JAO) on cell viability, oxidative stress and DNA damage was investigated in a myelo-monocytic cell line. Beyond confirming a microbiota imbalance in PC, we identified flour-specific effects: (i) reduction of *Veillonellaceae* with jatobá extract in PC samples; (ii) decrease in *Akkermansia* with jatoba and cumbaru flours; (iii) decreasing trend of *Faecalibacterium* and *Ruminococcus* with all flours tested, with the exception of the bocaiuva almond in HD samples for *Ruminococcus* and (iv) increase in *Lactobacillus* and *Bifidobacterium* in PC samples with bocaiuva almond flour. JAO displayed antioxidant properties protecting cells from daunorubicin-induced cytotoxicity, oxidative stress and DNA damage. The promising microbiota-modulating abilities of some flours and the chemopreventive effects of JAO deserve to be further explored in human intervention studies.

Keywords *Acrocomia aculeata*, *Dipteryx alata Vogel*, *Hymenaea courbaril*, short-chain fatty acids (SCFAs), antioxidants, gut microbiota.

Introduction

The Cerrado and Pantanal are biomes of South America that gather a great diversity of plant species. Among these plants, we can find many that have edible parts that could enrich the human diet. The fruit pulps and almonds of the Cerrado and Pantanal plants can be consumed raw or processed in the form of flours by local artisan food producers (Damasceno-Junior *et al.*, 2010). The jatobá pulp (*Hymenaea courbaril*), cumbaru almond (*Dypteryx alata* Vogel), bocaiuva almond (*Acrocomia aculeata*) and bocaiuva pulp are examples of materials for the manufacture of fruit flours, which can be sold in the local market, fairs and solidary economy shops. Cerrado and Pantanal fruits have great potential for economic growth due to their great diversity and nutritional content (Bortolotto *et al.*, 2017).

Brazilian Cerrado and Pantanal plants are influenced by climatic and geographical variations such as extreme temperature conditions, high incidence of UV radiation and occurrence of fires. As a result, these plants show adaptations such as high production of antioxidant enzymes and phenolic compounds (Arruda *et al.*, 2022). The nutritional composition of fruit flours may therefore exert beneficial effects after consumption. However, there is no scientific knowledge on the influence of their bioactive compounds on the human gut microbiota.

The human gut microbiota plays an important, multi-layered role in host physiology, including protection from infection and education and modulation of the immune system (Gibson *et al.*, 2017). Imbalances

*Correspondent: Email: silvia.turroni@unibo.it
Carolina Saori Ishii Mauro and Maryame Kadiri Hassani contributed equally.

doi:10.1111/ijfs.16274

in the gut microbiota (i.e., dysbiosis) can trigger inflammatory pathways in disease and have been linked to several gastrointestinal disorders, such as inflammatory bowel disease and irritable bowel syndrome, and to wider systemic manifestations, such as obesity, type 1 diabetes and atopy (Buford, 2017; Wilmes *et al*., 2022).

Recently, evidence has suggested distinct dysbiotic features in the gut microbiota of patients with coronavirus disease 2019 (COVID-19), which may persist in the long-term COVID-19 (Chhibber-Goel *et al*., 2021; Gaibani *et al*., 2021; Lau *et al*., 2022). Increases in microorganisms with pathogenic potential (e.g., *Enterococcus* and mucus degraders) and reductions of microorganisms with known immunomodulatory potential (e.g., short-chain fatty acid (SCFA) producers) have been reported up to 6 months after viral clearance (Liu *et al*., 2022). In this context, the regular consumption of probiotic, prebiotic food and products to modulate the gut microbiota could have relevant implications for the prevention and mitigation of COVID-19 (Lau *et al*., 2022).

Prebiotic is 'a substrate that is selectively utilised by host microorganisms conferring a health benefit' (Gibson *et al*., 2017). Currently established prebiotics are carbohydrates, oligo and polysaccharides, but other substances such as polyphenols and polyunsaturated fatty acids converted to their respective conjugated fatty acids may fit the definition if there is evidence in the target host (Gibson *et al*., 2017).

The consumption of fruit flours may also have effects on cell protection and oxidative stress prevention due to the content of antioxidants. Jatobá pulp extracts, fractions or compounds have shown antioxidant, anti-inflammatory, myorelaxant activities and anticancer properties (Jayaprakasam *et al*., 2007; Bezerra *et al*., 2013; Keiji *et al*., 1999).

In the present work, we used a gut model system, which simulated the human colon, to investigate the impact of four Brazilian fruit flours from Cerrado and Pantanal (i.e., jatobá pulp, cumbaru almond, bocaiuva pulp and bocaiuva almond) on gut microbiota composition and metabolic profile of healthy and post-COVID-19 subjects. Furthermore, we investigated the effect of jatobá pulp oil (JAO) on oxidative stress and DNA damage induced by a cytotoxic anthracycline (daunorubicin) in a myelo-monocytic cell line.

Materials and Methods

Characterisation of Cerrado and Pantanal fruit flours

The artisanal flours used in this study were obtained from the local market in the region of Mato Grosso do Sul, Brazil. The bocaiuva pulp and almond flours were obtained from the local market of Miranda (lat: 20° 14′ 34″ S, long: 56° 21′ 50″ W). The flours of jatobá and almond of cumbaru were purchased in the municipal market of Campo Grande (lat: 20° 26′ 34″ S, long: 54° 38′ 47″ W). To access the Genetic Heritage, this work was registered in the National System for the Management of Genetic Heritage and Associated Traditional Knowledge (SisGen, under n° A90CEAF).

The nutritional profile of the fruit flours was characterised by official reference methods (ashes: UNI ISO 2171; proteins: UNI 10274 831/12/93 and ISO 1871 (15/12/75)); total dietary fibre according to Lee *et al*. (1992). The energy value of the foods was estimated using the Atwater conversion factors (Merril & Watt, 1973).

The amino acid profile analysis was carried out according to AccQ-Tag Ultra Derivatization AminoAcids Kit (SKU: 186003836) UPLC® Amino Acid Analysis Application Solution (Waters, Wilmslow, UK).

pH-controlled batch culture systems

Stool sample collection and preparation

Faecal samples were donated by three individuals up to 10 days after SARS-CoV-2 clearance and by three healthy individuals. The samples were collected in an anaerobic jar (AnaeroJar™ 2.5 L, Oxoid Ltd.) including a gas-generating kit (AnaeroGen™, Oxoid). On the day of the experiment, each faecal sample (20 g) was diluted in 100 mL of anaerobic phosphate buffer solution (0.1 mol/L, pH 7.4, w/w) and homogenised (Stomacher 400, Seward, West Sussex, UK) for 2 min at 240 paddle beats per min. Samples were added to anaerobic fermenters within 15 min of voiding (Costabile *et al*., 2010).

In vitro batch culture fermentations

The flours were subjected to the simulated gastrointestinal digestion procedure as previously described by Guergoletto *et al*. (2016). Batch culture fermentation experimental condition, media composition and setting-up were carried out according to Corona *et al*. (2020).

Jatobá pulp flour (1% w/v), cumbaru almond flour (1% w/v), bocaiuva pulp flour (1% w/v) and bocaiuva almond flour (1% w/v) were fermented, along with inulin (Orafti® Inulin, BENEO, Germany) (1% w/v, positive control) and faecal slurry without any substrate addition (negative control). The plant-derived samples used in this part of the process were lyophilised digested flours, inoculated into the stirring batch-culture vessels containing faecal slurry (1%).

The experiment was carried out in triplicate, using a stool sample from a different donor each time. Flours or inulin were added to each container immediately

before adding 5 mL of faecal inoculum (1:10, w/v), to simulate the conditions of the distal region of the human large intestine (pH 6.7-6.9). Samples (4 mL) were collected at different time points (0, 4, 6 and 24 h) for microbiota profiling and metabolites analysis (see below). Samples were centrifuged for 20 min at 19,000× ***g*** and supernatant fractions were removed for SCFAs, ferric reducing antioxidant power assay (FRAP) and total phenolic content analysis (TPC), whereas the pellet was kept for microbial DNA extraction. All samples were stored at −80 °C prior to analysis.

Gut microbiota profiling through 16S rRNA amplicon sequencing

Microbial DNA was extracted from 250 mg of fermentation samples using the QIAamp DNA Stool Mini Kit (QIAGEN, Hilden, Germany) according to the manufacturer's instructions. The sequencing of the 16S rRNA gene was performed according to Corona *et al.* (2020). For each sample, the hypervariable V3–V4 regions of the 16S rRNA gene were PCR-amplified using the S-D-Bact-0341-b-S-17/S-D-Bact-0785-a-A-21 primers (Klindworth *et al.*, 2013) with Illumina overhang adapter sequences. Sequencing reads were deposited in the National Center for Biotechnology Information Sequence Read Archive (Bioproject ID: PRJNA913064) and sequences were processed using a pipeline combining PANDAseq (Masella *et al.*, 2012) and QIIME 2 (Bolyen *et al.*, 2019). After length and quality filtering, reads were binned into amplicon sequence variants (ASVs) using DADA2 (Callahan *et al.*, 2016). Taxonomy was assigned via the VSEARCH algorithm (Rognes *et al.*, 2016), using the Greengenes database as a reference. Alpha diversity was measured using the Shannon index and the number of observed ASVs. Beta diversity was computed based on weighted and unweighted UniFrac distances and visualised on a principal coordinates analysis (PCoA) plot.

Analysis of short-chain fatty acids

Acetic acid (C2), propionic acid (C3) and butyric acid (C4) were purchased from Merck (Darmstadt, Germany). All the stock solutions were prepared in water and stored at −20 °C. 4-Acetoamido-7-mercapto-2,1,3-benzoxadiazole (AABD-SH) was purchased from Biosynth Carbosynth Ltd. (Compton, UK). Triphenylphosphine (TPP), 2,2'-dipyridyl disulfide (DPDS) and mobile phase solvents were from Fisher Scientific UK Ltd. (Loughborough, UK).

Samples taken at 0, 4, 6 and 24 h were analysed for SCFA content. Fermentation supernatant samples were derivatised based on the method described by Song *et al.* (2019). Briefly, 380 µL of water and 20 µL of internal standard (where appropriate) were added to 200 µL of centrifuged stool samples and mixed well. The solution was transferred to a membrane filter (Microcon-30 kDa centrifugal filter unit with ultracel-30 membrane, Merck KGaA, Darmstadt, Germany) and centrifuged at 19,000× ***g*** for 20 min at 4 °C to remove any floating particulates in the supernatant. Afterwards, the supernatants were collected to perform the derivatisation.

For derivatisation of SCFAs, 20 µL each of 20 mM AABD-SH, 20 mM TPP and 20 mM DPDS in dichloromethane were added to the supernatant and derivatisation was performed at room temperature for 5 min while vortexing. The reaction solution was dried under nitrogen, and then reconstituted with 200 µL methanol prior to UPLC-MS/MS analysis. The calibration curves were generated with standard solutions (100 nM to 1 mM). Derivatives were measured on the UPLC MS/MS system consisting of an Aquity UPLC H-Class coupled to a Xevo TQ-S micro-ESI mass spectrometer (both Waters, Wilmslow, UK). Separation was achieved on the HSS T3 column (1.8 µm, 2.1 × 100 mm) with an HSS T3 VanGuard column (both Waters) held at 45 °C with mobile phase A (water + 0.1 % formic acid) and mobile phase B (acetonitrile + 0.1% formic acid) at a flow rate of 0.6 mL/min and a gradient of initial 99% A for 1 min, followed by a linear decrease to 5% A after 5 min, held at 5% until 6.5 min, switched back to 99% A at 6.55 min, held until 8 min. Mass spectrometry was conducted in positive ion mode with an ionisation voltage of 3.5 kV and desolvation gas flow of 650 L/h at a temperature of 450 °C. Transitions were taken from Song *et al.* (2019). Data analysis, including baseline correction and QC batch correction, was carried out in Matlab using in-house scripts (modified from Behrends *et al.* (2011)).

Total Phenolic Content and Ferric Reducing Antioxidant Power

During fermentation, aliquots were taken at 0 and 24 h to access the TPC and the *in vitro* antioxidant activity. The TPC was determined spectrophotometrically using the Folin–Ciocalteau assay (Swain & Hills, 1959). The results were expressed as mM gallic acid equivalent (mM GAE). To assess the antioxidant activity, FRAP was determined (Benzie & Strain, 1996). The results were expressed as µM ascorbic acid equivalent (µM AAE). Both methods had the volumes adapted to a 96-well plate and read in a microplate reader (Thermo Scientific Multiskan EX).

Effect of the jatobá pulp oil on cell viability, oxidative stress and DNA damage

Prior to cell culture analysis, the JAO was extracted according to Bligh & Dyer (1959).

Cell culture

The acute myeloid leukaemia cell line MV411 cell line (ATCC) was grown in 90% RPMI 1640 medium (Sigma R8758) supplemented with 10% FBS (Fisher 11550356) and 1% pen/strep (Sigma P4333) at 37 °C with 5% CO_2 and 95% humidity. The cells were stably infected with a lentivirus vector expressing the green fluorescent protein (GFP) (Arroyo and Calle, unpublished data). The parental cell line was used for the immunofluorescence experiments whereas the GFP cell line was used for the cytotoxic and oxidative stress experiments.

Cytotoxic, oxidative stress and DNA damage assay

For the cell viability and oxidative stress experiments, MV411-eGFP cells were seeded in 96-well plates (flat bottom) (4×10^4 cells/200 µl/well) and incubated at 37 °C with 5% CO_2 and 95% humidity. After 24 h, the cells were divided 1:2 and treated with serial ten-fold dilutions of JAO (from 37.5 µg/mL to 3.75 ng/mL) or vehicle (dimethyl sulfoxide – DMSO) for 24 h. After 24 h, daunorubicin (25 nM) was added to half of the wells and the plate was incubated at 37 °C with 5% CO_2 and 95% humidity for another 24 h. The day after, Cell Rox (250 nM) (Thermofisher) was added to the appropriate wells and the plate was incubated for 1 h at 37 °C with 5% CO_2 and 95% humidity in the dark. The plate was analysed by flow cytometry using a BD Accuri™ C6 Flow cytometer to discriminate GFP-(dead cells) from GFP (alive cells) and detect oxidative stress within the samples by measuring the fluorescence emitted by Cell Rox. For the DNA damage experiments, MV411-cells were seeded in 24-well plates (1.6×10^5 cells/1 mL/well) and incubated at 37 °C with 5% CO_2 and 95% humidity. After 24 h, the cells were divided 1:2 and treated with JAO (37.5 ng/mL) or vehicle (DMSO) for 24 h. After 24 h, daunorubicin (25 nM) was added to half of the appropriate wells and the plate was incubated at 37 °C with 5% CO_2 and 95% humidity for another 24–48 h, when the cells were collected for analysis of DNA damage.

Flow cytometry

The samples were processed for analysis of apoptosis/viability and oxidative stress by flow cytometry BD Accuri™ C6, using the GFP signal, measured in the FL1-A channel (533/30) and Cell Rox, measured in the FL4-A channel (780/605). The cell population was identified and gated based on the forward and side scatter signals profile (FSC/SSC). The combination of these two parameters allows for the discrimination of the cells by size and internal complexity in single-cell analysis. Among this population, we performed doublets discrimination by plotting area (-A) against the height (-H) for the forward scatter (FSC-A vs. FSC-H). Doublets present double the area and width values of single cells whilst the height is roughly the same. Disproportions between height and area are used to identify doublets. This accurate discrimination ensures the exclusion of false fluorescence emission. For each cell population, we recorded a minimum of 10,000 events in a medium flow rate in the ungated sample. Results were given in percentage of GFP positive cells (M6 population) and median fluorescence intensity (MFI) for Cell Rox. The cleaning and validations of the flow cytometry were done before each use. Firstly, the cleaning was done with 10% bleach for 2 min, then the rinsing was done with water for 2 min. Finally, the first validation was done with Spherotech 8-Peak validation beads and the second one with Spherotech 6-Peak validation beads.

Analysis of DNA damage by immunofluorescence

Analysis of DNA damage was performed as described (Esposito *et al.*, 2015). Briefly, the cells were transferred from the wells to individual Eppendorf tubes, then centrifuged for 5 min at 500× ***g***. After that, the supernatant was discarded, and the pellet was resuspended in 200 µL of PBS and half of the cells were spun for 5 min at 300× ***g*** on a glass slide using a cytospin cytocentrifuge. Following that, the slides were fixed in 4% paraformaldehyde for 15 min and washed three times with PBS 1× for 5 min. The cells were permeabilised and blocked in 10% FBS/1% BSA/0.5% TX-100/TBS 1× for 15 min. Then, the slides were washed three times in cold PBS 1× and incubated with the primary antibody mouse anti yH2AX (1:200) in 10%FBS/1% BSA/TBS 1× and incubated in the dark overnight at 4 °C. The day after, the slides were washed three times with PBS 1× for 5 min to remove the primary antibody. The slides were then incubated with the secondary antibody Donkey anti-mouse DL 488 Jackson/Stratech 715-485-150 (1:200) in DAPI 0.2 µg/mL/10%FBS/1% BA/TBS 1× in the dark for 1 h. The slides were washed three times for 10 min with PBS 1×/0.05% Tween 2, then mounted with Mowiol-DABCO, by adding 1 drop of mounting medium on the edge of the cells and covered with the coverslip. The slides were stored at room temperature for 24 h and then examined under the microscope. Pictures were captured using Evos FL Digital Inverted Fluorescence Microscope.

Statistical analysis

The fruit flour characterisation, TPC and FRAP data were submitted to analysis of variance (ANOVA) and Tukey's test, for comparison of means at the level of 5% of significance, using the STATISTICA 12.0 program (StatSoft Inc., Tulsa, OK). The cell culture data were submitted to a 2-Way ANOVA Sidak's multiple

comparison test for oxidative stress induced by daunorubicin or 2-Way ANOVA Tukey's multiple comparison test for the cytotoxic effect of daunorubicin and DNA damage. The figures were developed in GraphPadPrism 8 (GraphPad Software, San Diego, CA).

As for the microbiota data, the statistical analysis was performed using R Studio 1.0.44 on R software version 3.3.2 (https://www.r-project.org) implemented with the R packages stats and vegan (https://cran.r-project.org/web/packages/vegan). The significance of data separation in the PCoA plot was tested by PERMANOVA using the function adonis in vegan. Bar plots were built using the R package made4 (Culhane *et al*., 2005). Non-parametric tests (Kruskal–Wallis test or Wilcoxon test) were used to assess differences in alpha diversity and relative taxon abundance. Kendall rank correlation test was used to assess the associations between genus-level relative abundances and SCFA levels. A P-value ≤ 0.05 was considered statistically significant; a P-value between 0.05 and 0.2 was considered a trend.

Results

Characterisation of Cerrado and Pantanal fruit flours

The tested flours showed differences in terms of macronutrient composition, especially because they were derived either from the almond or from the pulp of fruits (Table 1). All flours showed moisture below 10% (w/w), which is a desirable stability indicator since the low moisture content prevents enzymatic activity and undesirable microbial growth.

The Jatobá pulp flour presented 44.49 g/100 g of fibre, a higher value compared to the other flours, which was also reflected in higher values of both soluble and insoluble fibres ($P < 0.05$). Cumbaru almond flour presented the highest protein content, with 25.70 g/100 g ($P < 0.05$). The flours made of almonds had high lipid content of 61.18 g/100 g and 41.21 g/100 g for bocaiuva almond and cumbaru almond flour, respectively. All flours are calorie-dense food, however, bocaiuva almond flour stood out as having the highest energy value, especially due to its high lipid content.

Regarding essential amino acids, cumbaru almond flour, bocaiuva pulp and bocaiuva almond flour presented scores 3.03, 7 and 6.3 times higher, respectively, when compared to jatobá pulp flour. The bocaiuva pulp and bocaiuva almond flours did not differ from each other in terms of essential amino acids, however, bocaiuva almond flour showed higher levels of tryptophan, threonine and lysine, while bocaiuva pulp flour had higher levels of leucine, isoleucine and phenylalanine.

The amino acid profile showed that jatobá fruit flour has a higher content of the non-essential amino acids proline and asparagine. Cumbaru almond flour presented the highest concentrations of the non-essential amino acids aspartate and glutamate ($P < 0.05$). Serine and glutamine levels did not differ for all fruit flour samples ($P > 0.05$).

Colonic fermentation system

Impact on faecal-derived microbial communities

The 16S rRNA gene-based next-generation sequencing of all fermentation samples yielded a total of 2,142,849 high-quality reads, with an average of 14,881 ± 4,498 sequences per sample, binned into 4,849 ASVs.

No significant differences were observed in alpha diversity across the entire dataset, regardless of the origin of the faecal sample (post-COVID-19 – PC, or healthy donor – HD), experimental condition (fruit flours, inulin and negative control) and time point (0, 4, 6 and 24 h of fermentation – T0, T4, T6 and T24) ($P > 0.05$, Wilcoxon test). However, it should be noted that the diversity of both PC and HD faecal-derived microbial communities tended to decrease over time in all experimental conditions (Figure S1).

As for beta diversity, the PCoA of inter-sample variation based on weighted (Figure 1) and unweighted (Figure S2) UniFrac distances showed significant segregation between PC and HD faecal-derived microbial communities, regardless of experimental condition and time point ($P < 0.001$, PERMANOVA), thus suggesting the existence of distinctive features of the microbiota at baseline and over time. When focusing on each group (PC and HD), we found that the samples were significantly separated by experimental condition and time point ($P < 0.001$), underlining a differential impact of fruit flours over time. Interestingly, such an impact was overall more marked than that of inulin and negative control.

From the taxonomic standpoint, the differences between the PC and HD faecal-derived microbial communities at baseline were mostly attributable to decreased relative abundances of some Firmicutes members, namely *Christensenellaceae* and *Ruminococcus*, and *Akkermansia* in the former, along with increased proportions of *Faecalibacterium*, *Veillonella* and unclassified *Lachnospiraceae* ($P \leq 0.05$, Wilcoxon test) (Figure 2). Regarding the impact of fruit flours, we observed both common and peculiar microbial signatures of response (Figure 3). Among the features shared between PC and HD, it is worth noting that 24 h of fermentation with the fruit flours resulted in decreased proportions of *Lachnospiraceae* and *Ruminococcaceae*, and increased amounts of *Enterobacteriaceae* ($P \leq 0.2$). Although in the absence of statistical significance, these variations were also observed in the control vessels (i.e., with the addition of inulin or without any

Table 1 Proximate composition and amino acid profile of Cerrado and Pantanal fruit flours. Data are presented as mean ± standard deviation ($n = 3$)

	Jatobá pulp	Cumbaru almond	Bocaiuva pulp	Bocaiuva almond
Component (g/100 g)				
Moisture	$8.30^{A} \pm 0.11$	$4.90^{B} \pm 0.70$	$8.60^{A} \pm 0.08$	$5.60^{B} \pm 0.10$
Ash	$3.60^{A} \pm 0.10$	$2.70^{B} \pm 0.10$	$3.80^{A} \pm 0.09$	$1.80^{C} \pm 0.04$
Protein	$7.40^{C} \pm 0.25$	$25.70^{A} \pm 0.60$	$3.20^{D} \pm 0.70$	$12.50^{B} \pm 0.40$
Lipid	$3.05^{D} \pm 0.30$	$41.21^{B} \pm 0.80$	$19.46^{C} \pm 0.50$	$61.18^{A} \pm 0.40$
Carbohydrate	$33.16^{B} \pm 0.57$	$3.42^{C} \pm 0.85$	$38.55^{A} \pm 0.90$	$1.62^{C} \pm 0.60$
Total fibre	$44.49^{A} \pm 0.39$	$22.07^{C} \pm 1.28$	$26.39^{B} \pm 1.10$	$17.13^{D} \pm 0.80$
Soluble fibre	$11.13^{A} \pm 0.27$	$2.32^{C} \pm 0.37$	$8.85^{B} \pm 0.70$	$1.80^{C} \pm 0.38$
Insoluble fibre	$33.36^{A} \pm 0.60$	$19.75^{B} \pm 1.47$	$16.54^{C} \pm 1.00$	$15.76^{C} \pm 1.40$
Energy value (kcal/100 g)	$189.70^{D} \pm 2.40$	$487.31^{B} \pm 2.91$	$342.14^{C} \pm 6.39$	$607.10^{A} \pm 8.20$
Amino acid profile (mg/g protein)				
Glycine	$2.83^{B,C} \pm 0.78$	$8.8^{A,B} \pm 0.59$	$1.8^{C} \pm 0.86$	$10.0^{A} \pm 2.00$
Lysine*	$2.6^{C} \pm 0.32$	$36.9^{B} \pm 0.05$	$3.3^{C} \pm 0.51$	$49.0^{A} \pm 2.68$
Alanine	$22.5^{B} \pm 2.51$	$33.4^{B} \pm 1.55$	$44.9^{B} \pm 2.45$	$75.2^{A} \pm 9.53$
GABA	$1.4^{C} \pm 0.21$	$5.3^{B,C} \pm 0.49$	$32.5^{A} \pm 1.76$	$10.9^{B} \pm 0.94$
Serine	$45.4^{A} \pm 0.52$	$21.1^{A} \pm 0.70$	$22.5^{A} \pm 5.33$	$42.1^{A} \pm 6.83$
Proline	$345.4^{A} \pm 7.32$	$23.7^{B} \pm 3.56$	$14.6^{B} \pm 0.64$	$10.6^{B} \pm 1.73$
Asparagine	$446.1^{A} \pm 5.02$	$73.0^{B} \pm 2.13$	$18.2^{D} \pm 1.28$	$48.9^{C} \pm 2.03$
Glutamine	$1.4^{A} \pm 0.25$	$0.2^{A} \pm 0.06$	$2.8^{A} \pm 1.23$	$2.0^{A} \pm 0.70$
Aspartate	$27.0^{C} \pm 0.68$	$128.4^{A} \pm 7.36$	$67.0^{B} \pm 2.11$	$45.3^{B,C} \pm 3.71$
Glutamate	$7.0^{C} \pm 0.71$	$418.8^{A} \pm 4.41$	$42.8^{C} \pm 5.09$	$175.2^{B} \pm 10.72$
Threonine*	$25.1^{A,B} \pm 0.29$	$12.9^{B} \pm 0.11$	$15.7^{B} \pm 0.22$	$40.8^{A} \pm 6.49$
Homoserine 3	n.d.	$0.2^{B} \pm 0.10$	$1.2^{A} \pm 0.09$	$0.3^{B} \pm 0.01$
Methionine*	n.d.	$1.2^{B} \pm 0.07$	n.d.	$12.2^{A} \pm 0.29$
Valine*	$23.3^{C} \pm 4.35$	$49.9^{B,C} \pm 1.51$	$153.9^{A} \pm 28.17$	$118.6^{A,B} \pm 0.43$
Leucine*	$6.6^{C} \pm 0.25$	$31.2^{C} \pm 0.57$	$184.5^{A} \pm 9.52$	$92.5^{B} \pm 5.29$
Isoleucine*	$5.1^{D} \pm 0.60$	$50.4^{C} \pm 1.11$	$136.9^{A} \pm 4.87$	$116.7^{B} \pm 4.44$
Histidine*	$1.2^{A} \pm 0.35$	$1.6^{A} \pm 0.17$	n.d.	$0.4^{A} \pm 0.03$
Aminoadipate	$0.9^{B} \pm 0.08$	$0.1^{B} \pm 0.08$	$109.5^{A} \pm 3.86$	$1.5^{B} \pm 0.33$
Phenylalanine*	$8.4^{D} \pm 0.44$	$64.0^{C} \pm 4.27$	$102.6^{A} \pm 5.21$	$82.3^{B.C} \pm 5.42$
Arginine	$6.5^{A} \pm 0.35$	8.5 ± 0.37	$6.0^{A} \pm 0.74$	$2.1^{B} \pm 0.71$
Citrulline	$0.3^{A} \pm 0.03$	$0.5^{A} \pm 0.02$	n.d.	$0.6^{A} \pm 0.02$
Tyrosine	$5.7^{C} \pm 1.63$	$14.3^{B,C} \pm 0.61$	$28.6^{A} \pm 2.05$	$23.8^{A,B} \pm 4.05$
Tryptophane*	$15.4^{B} \pm 0.87$	$15.6^{B} \pm 2.37$	$10.8^{B} \pm 2.99$	$39.0^{A} \pm 0.71$
Essential amino acid score (%)	$8.8^{C} \pm 1.1$	$26.4^{B} \pm 1.4$	$60.9^{A} \pm 7.3$	$55.2^{A} \pm 3.6$

$^{A\text{-}D}$Different uppercase letters within a row indicate significant differences ($P < 0.05$).

GABA, gamma-aminobutyric acid; n.d., not detected.

*Essential amino acids.

extract – negative control). When looking for fruit flour-specific effects, we observed: (i) a reduction of *Veillonellaceae* with jatobá extract in PC samples; (ii) a decrease in *Akkermansia* with jatoba and cumbaru flours; (iii) a decreasing trend of *Faecalibacterium* and *Ruminococcus* in the presence of all flours tested, with the exception of the bocaiuva almond in HD samples for *Ruminococcus*; and (iv) an increase in *Lactobacillus* and *Bifidobacterium* in PC samples with bocaiuva almond flour ($P \leq 0.2$).

Analysis of short-chain fatty acids

Table 2 shows the concentrations of the major SCFAs at 0, 4, 6 and 24 h of fermentation with fruit flours, inulin and negative control. Overall, SCFA concentrations tended to increase after 24-h fermentation due to substrate utilisation by gut bacteria. Jatobá pulp flour generated higher butyrate production when compared to the other flours in HD ($P < 0.05$), whereas no changes were observed in PC. None of the flours generated major changes in propionate production in both donors. No significant correlations were found between SCFA levels and genus-level relative abundances during fermentation ($P > 0.05$, Kendall rank correlation test).

Total Phenolic Content and Ferric Reducing Power

To measure the antioxidant activity during colonic fermentation, the TPC content and FRAP were

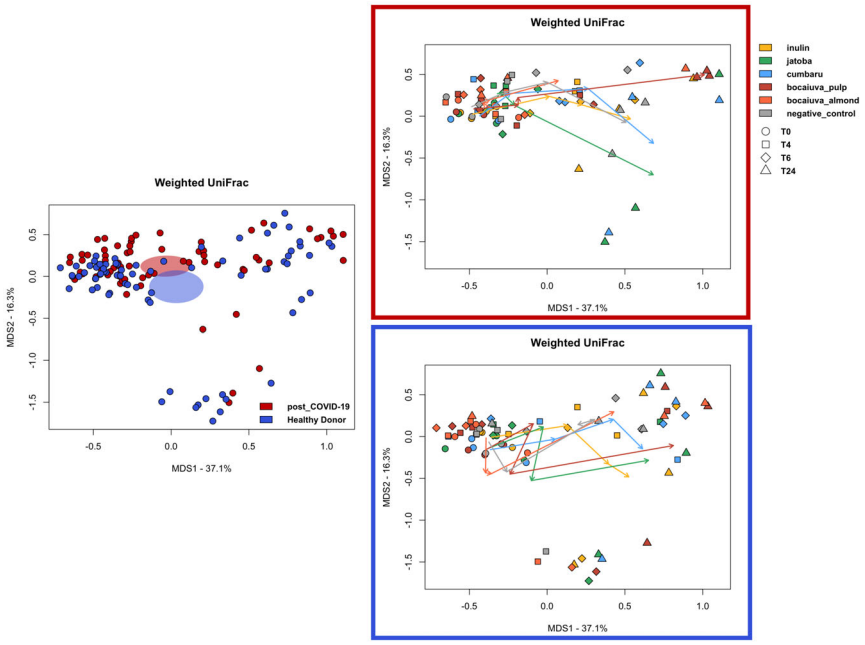

Figure 1 Faecal-derived microbial communities of post-COVID-19 donors separate from those of healthy donors in 24-h fermentation experiments in the presence of fruit flours, inulin or without additions. Left, principal coordinates analysis (PCoA) based on weighted UniFrac distances, showing all fermentation samples, coloured by a group of donors (post-COVID-19 donors, PC, red vs. healthy donors, HD, blue). A significant separation between groups was found, regardless of experimental condition (fruit flours, inulin and negative control) and time point (0, 4, 6 and 24 h of fermentation – T0, T4, T6 and T24) ($P < 0.001$, PERMANOVA). Right, PCoA plots show the fermentation samples for PC (top panel) and HD (bottom panel). Within each group of donors, the samples were separated significantly by experimental condition (fruit flours, inulin and negative control) and time point (T0, T4, T6 and T24) ($P < 0.001$).

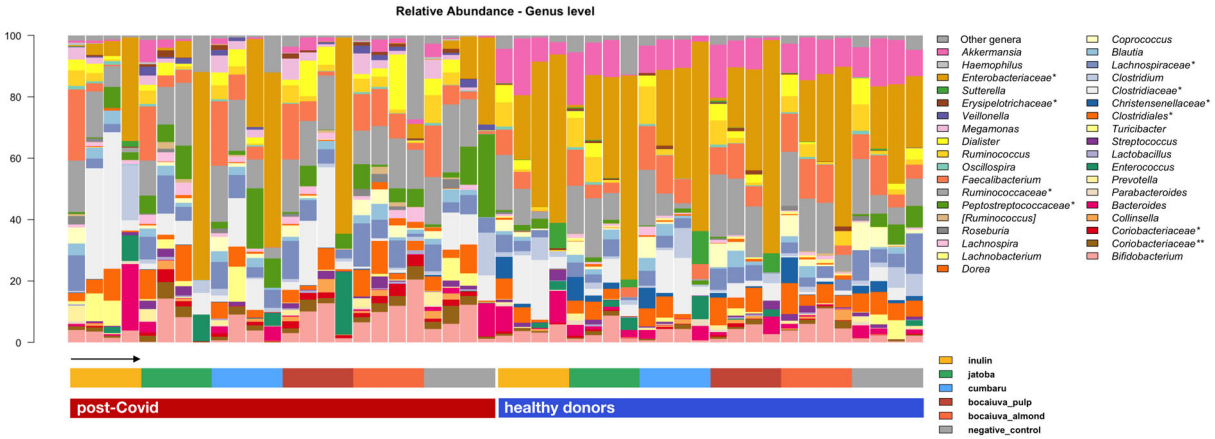

Figure 2 Genus-level relative abundance profiles of faecal-derived microbial communities of post-COVID-19 and healthy donors at 0, 4, 6 and 24 h of fermentation in the presence of fruit flours, inulin or without additions. *, unclassified amplicon sequence variants reported at higher taxonomic level; **, other. For each group of donors (post-COVID-19, PC and healthy donors, HD), the profiles are shown in the following order: samples at 0, 4, 6 and 24 h fermentation (T0, T4, T6 and T24) in the presence of inulin (yellow), jatobá (green), cumbaru (light blue), bocaiuva pulp (red), bocaiuva almond (orange) and negative control (grey). The black arrow below the histograms indicates the temporal succession for each quadruplet of samples (T0, T4, T6 and T24).

monitored (Figures 4 and 5). As regards the fermentation process, no differences were found for TPC over time. On the other hand, FRAP analysis showed an increase in antioxidant activity after 24 h for jatobá pulp and bocaiuva pulp flours exclusively in PC ($P < 0.05$). The other treatments did not result in significant differences in FRAP for either HD or PC ($P < 0.05$).

However, it was possible to observe an increase in TPC at T0 in the treatments with the fruit flour samples when compared to the negative control and even to the inulin treatment (positive control). This was due

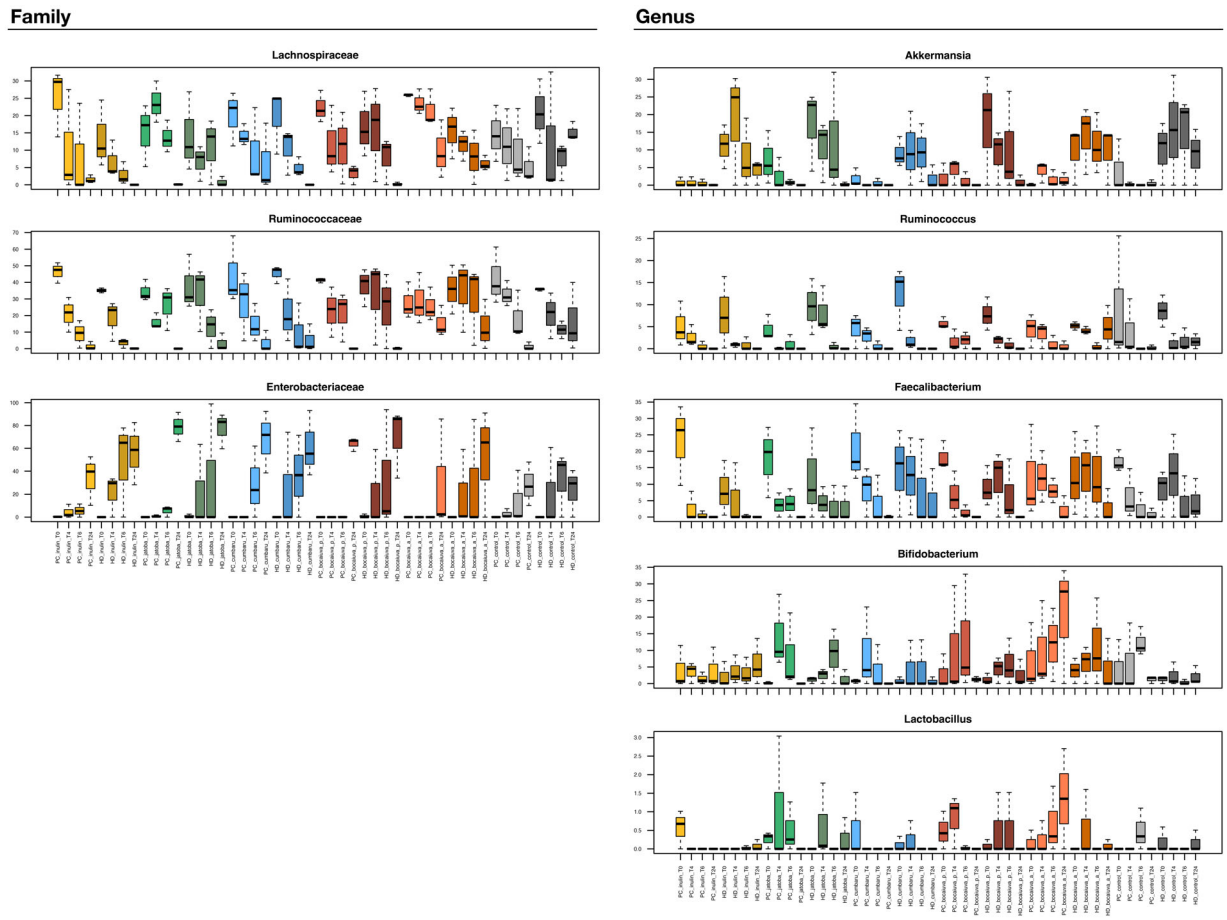

Figure 3 Families and genera of faecal-derived microbial communities of post-COVID-19 (PC) and healthy donors (HD), differing over time in 24-h fermentation experiments in the presence of fruit flours, inulin or without additions. Boxplots showing the relative abundance distribution of bacterial taxa in the different study groups at 0, 4, 6 and 24 h fermentation (T0, T4, T6 and T24). Only significantly different taxa or trends are shown ($P \leq 0.2$, Wilcoxon test). Bocaiuva_p, bocaiuva pulp; bocaiuva_a, bocaiuva almond; control, without any additions.

to the presence of phenolic compounds in these fruit flours.

Effect of the jatobá pulp oil on cell viability, oxidative stress, and DNA damage

We tested the antioxidant properties of JAO in a myelo-monocytic cell line (MV411-eGFP), engineered to express enhanced GFP (eGFP), as described in the materials and methods. We first determined the half-maximal inhibitory concentration (IC50) for JAO by incubating the cells with escalating concentrations of JAO extract and measuring the percentage of eGFP-positive (alive) and negative cells (dead). The results indicated that the IC50 for JAO in MV411 is 71 μg/mL (Figure 6a). We then decided to assess the effect of non-toxic and non-pharmacological concentrations of JAO (ranging from 3.75 ng/mL to 37.5 μg/mL) on oxidative stress and DNA damage induced by daunorubicin, an anthracycline antibiotic widely used in chemotherapy, which possesses several mechanisms of action, including intercalation into DNA strands, topoisomerase II inhibition, formation of DNA double-strand breaks and production of reactive oxygen species (ROS) (Al-Aamriri *et al.*, 2019). Following exposure of MV411 cells to daunorubicin, a significant increase in oxidative stress, measured as fluorescence emitted by Cell ROX, was observed (MFI Cell ROX in vehicle vs. daunorubicin, 249912.292± 93116.016 vs. 356684.786±117841.971, $P < 0.05$; fold increase, 1.42±0.47) (Figure 6b and Figure S3). This was accompanied by a cytotoxic effect (fraction of eGFP-cells in vehicle vs. daunorubicin, 0.084 ± 0.028 vs. 0.242 ± 0.185, $P < 0.05$; fold increase, 2.88 ± 2.2) (Figure 6c and Figure S3). Twenty-four hours pre-exposure with JAO extract reduced daunorubicin-

Table 2 Concentrations of major short-chain fatty acids (acetate, propionate and butyrate) at 0, 4, 6 and 24 h of fermentation of Brazilian fruit flours, inulin and negative control in stirred pH-controlled batch culture systems with stool samples from healthy (HD) and post-COVID-19 donors (PC). Data are presented as mean ± standard deviation ($n = 3$)

Treatment	Time point (h)	HD			PC		
		Acetate	Propionate	Butyrate	Acetate	Propionate	Butyrate
Inulin (positive control)	0	4.28 ± 0.25	3.77 ± 0.05	4.74 ± 0.28	4.12 ± 0.48	3.75 ± 0.29	5.26 ± 0.06
	4	4.28 ± 0.46	3.61 ± 0.11	4.85 ± 0.25	4.93 ± 0.44	4.54* ± 0.24	5.65 ± 0.26
	6	4.63 ± 0.15	3.58 ± 0.27	4.69 ± 0.50	4.95* ± 0.17	4.40* ± 0.11	5.59* ± 0.16
	24	5.40^{*A} ± 0.24	4.98^{*A} ± 0.23	7.21^{*A} ± 0.43	$5.15^{*A,B}$ ± 0.24	4.73^{*A} ± 0.02	6.68^{*A} ± 0.20
Jatobá pulp flour	0	4.10 ± 0.0	3.41 ± 0.00	4.79 ± 0.14	3.74 ± 0.05	4.19 ± 0.01	5.72 ± 0.39
	4	3.87 ± 0.43	3.55 ± 0.43	4.89 ± 0.30	4.25* ± 0.27	4.43* ± 0.11	5.61 ± 0.36
	6	3.99 ± 0.36	3.43 ± 0.08	5.07 ± 0.45	4.50* ± 0.31	3.91 ± 0.71	5.60 ± 0.10
	24	$4.78^{A,B}$ ± 0.52	$4.01^{A,B,C}$ ± 0.59	$6.38^{*A,B}$ ± 0.19	4.59^{*C} ± 0.44	3.99^{A} ± 0.34	$5.74^{A,B}$ ± 0.16
Cumbaru almond flour	0	3.61 ± 0.01	2.81 ± 0.00	4.55 ± 0.24	3.08 ± 0.33	3.03 ± 0.42	4.70 ± 0.12
	4	4.01 ± 0.42	2.96* ± 0.04	4.58 ± 0.41	3.20 ± 0.18	2.63 ± 0.10	4.43 ± 0.41
	6	3.74* ± 0.02	2.94 ± 0.15	4.44 ± 0.19	4.20* ± 0.26	3.83* ± 0.63	5.46* ± 0.29
	24	3.90^{B} ± 0.40	$3.39^{*B,C}$ ± 0.33	$5.36^{*B,C}$ ± 0.61	$4.21^{*B,C}$ ± 0.27	4.01^{*A} ± 0.42	4.81^{B} ± 0.03
Bocaiuva pulp flour	0	4.29 ± 0.02	3.32 ± 0.40	4.80 ± 0.20	4.28 ± 0.19	3.07 ± 0.06	4.82 ± 0.25
	4	4.03 ± 0.28	3.49 ± 0.05	4.70 ± 0.24	4.36 ± 0.32	3.94* ± 0.34	5.19 ± 0.45
	6	4.05* ± 0.18	3.38 ± 0.25	4.59 ± 0.06	4.18 ± 0.34	3.53 ± 0.47	5.33 ± 0.36
	24	$4.5^{A,B}$ ± 0.30	$3.30^{B,C}$ ± 0.27	$5.5^{*B,C}$ ± 0.42	$4.55^{B,C}$ ± 0.08	3.70^{*A} ± 0.19	5.07^{B} ± 0.30
Bocaiuva almond flour	0	3.05 ± 0.20	3.27 ± 0.27	4.52 ± 0.15	4.77 ± 0.75	4.19 ± 0.22	5.09 ± 0.13
	4	4.34* ± 0.29	3.49 ± 0.37	4.73* ± 0.15	5.60 ± 0.05	4.08 ± 0.68	4.83 ± 0.30
	6	4.36* ± 0.32	3.38 ± 0.50	4.59 ± 0.30	5.36 ± 0.12	4.22 ± 0.17	5.14 ± 0.32
	24	4.27^{*B} ± 0.22	3.15^{C} ± 0.13	$4.56^{C,D}$ ± 0.27	5.67^{A} ± 0.17	4.68^{A} ± 0.94	$5.56^{A,B}$ ± 1.19
Negative control	0	4.10 ± 0.34	3.45 ± 0.01	4.57 ± 0.01	3.43 ± 0.49	3.51 ± 0.69	4.57 ± 0.09
	4	3.90 ± 0.01	3.36 ± 0.09	4.80 ± 0.08	4.35* ± 0.22	3.90 ± 0.04	5.43* ± 0.04
	6	4.33 ± 0.26	4.37* ± 1.05	4.09 ± 0.90	4.54 ± 0.28	4.08 ± 0.24	5.56* ± 0.12
	24	$4.79^{*A,B}$ ± 0.54	$4.49^{*A,B}$ ± 0.84	4.27^{*D} ± 0.24	$4.63^{*B,C}$ ± 0.31	4.42^{A} ± 0.51	5.24^{*B} ± 0.10

$^{A-D}$Significant differences of each SCFA at 24 h of fermentation using one-way ANOVA with Tukey's post-hoc comparison ($P < 0.05$).
*Significant differences compared to baseline (0 h) within the same substrate (using *t*-test, $P < 0.05$).

induced oxidative stress and cytotoxic effect to levels comparable to the vehicle (DMSO) (Figure 6b and c and Figure S3), demonstrating a chemopreventive effect against daunorubicin-induced cytotoxic effect and oxidative stress.

Incubation with daunorubicin also induced a significant increase in DNA damage (double-strand breaks), measured as the percentage of cells showing more than 6 γH2AX foci (% cells with >6γH2AX foci in vehicle vs. daunorubicin after 48-h exposure, 0 ± 0 vs. 54.95 ± 11.07, $P < 0.05$) (Figure 6d and e). Twenty-four hours pre-exposure with JAO (37 ng/mL) reduced daunorubicin-induced DNA damage to levels comparable to vehicle (DMSO) (% cells with >6γH2AX foci in vehicle vs. JAO after 24-h exposure, 0 ± 0 vs. 5.55 ± 9.62, $P = 0.34$; daunorubicin vs. daunorubicin+JAO after 24-h exposure, 54.95 ± 11.07 vs. 9.34 ± 8.94, $P < 0.01$) (Figure 6d and e and Figure S4), demonstrating that JAO pulp exerted a chemopreventive effect even against daunorubicin-induced DNA damage.

Discussion

The Brazilian pulp and almond fruit flours tested in this study presented important nutritional values, with proteins, sugars, fibre, and lipids. The total fibre in jatobá pulp flour was present in greater quantity than in other flours, which may contribute to a beneficial activity for use by gut bacteria (Gibson *et al.*, 2017). Bocaiuva almond flour had the highest lipid content, even when compared to *in natura* bocaiuva almond in the literature (Hiane *et al.*, 2006). Bocaiuva pulp and almond flour were also potentially good sources of some essential amino acids, as they had a higher essential amino acid score than other flours. However, for a protein to be considered of good quality, it must be well absorbed after digestion. To assess this, a direct study by measuring nitrogen balance along with body weight and body composition is required (Joint WHO/FAO/UNU, 2007). The protein content and amino acid profile of foods are important substrates for gut fermentation, as they provide nitrogen sources for the

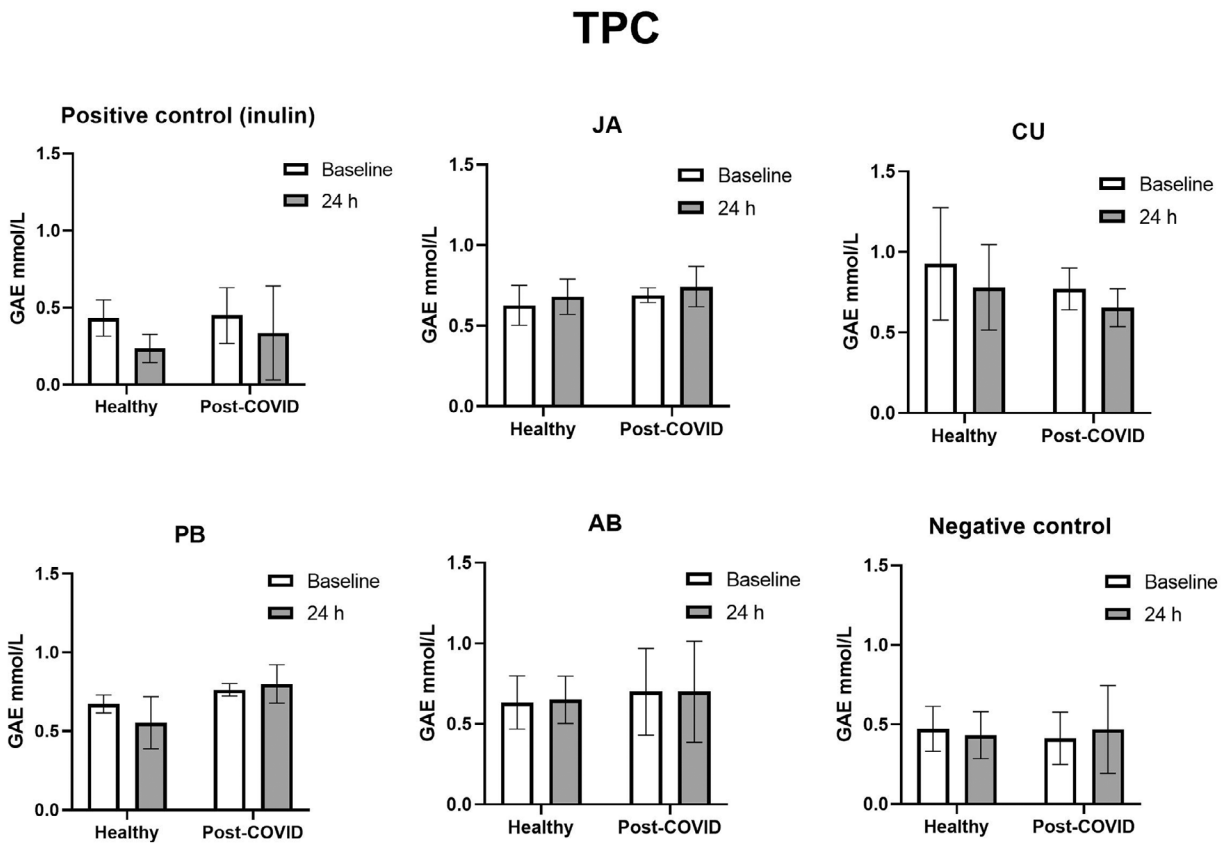

Figure 4 Total phenolic content (mM gallic acid equivalent – GAE) of the supernatants collected at baseline and after 24 h of in vitro colonic fermentation of Brazilian fruit flours, inulin and negative control with stool samples from healthy and post-COVID-19 donors. AB, bocaiúva almond flour; CU, cumbaru almond flour; GAE, gallic acid equivalent; JA, jatobá pulp flour; PB, bocaiuva pulp flour.

proliferation of bacteria. It has been suggested that specific amino acid mixtures are likely to be of benefit to the human colonic microbiota, in addition to dietary fibre and prebiotics (Bifari *et al*., 2017).

The small intestine is highly specialised in the breakdown, emulsification and absorption of nutrients and few nutrients escape the digestive process. The human body lacks the enzymes necessary to digest the wide range of complex carbohydrates allowing them to escape digestion in the small intestine. In the colon, however, they can be used as an energy source by specific resident bacteria (Louis & Flint, 2009; de Vos *et al*., 2022). Indeed, various gut microbes contribute to the metabolisation of these non-digestible polysaccharides into several endpoints of anaerobic fermentation, including SCFAs. These compounds regulate numerous metabolic pathways both in the intestine and at a distant level, that is, at the level of the liver, adipose tissue, muscles, and brain. It is in fact well known that SCFAs contribute to numerous physiological effects, ranging from modulation of energy homeostasis, glucose/lipid metabolism, inflammation and even immunity and cancer (Pascale *et al*., 2018; Silva *et al*., 2020; Marrocco *et al*., 2022).

Colonic fermentation models provide insights into the processes in the gut and are considered screening tools for many dietary ingredients. In this study, we chose to ferment fruit flours of pulp and almonds from Cerrado and Pantanal to observe the effect of these whole foods on microbiota modulation and production of SCFAs. Under these circumstances, the intention of these experiments was to use the food as it is sold in the local market and ready for consumption, considering all its characteristics of macronutrients that can positively impact the health of consumers. However, we are aware that it has been documented in the literature that the proximate composition of foods can directly affect the composition of the microbiota (Leeming *et al*., 2021). It should also be said that due to experimental constraints (mainly the working volume of our gut model system), we did not monitor changes in macronutrients and amino acid profile,

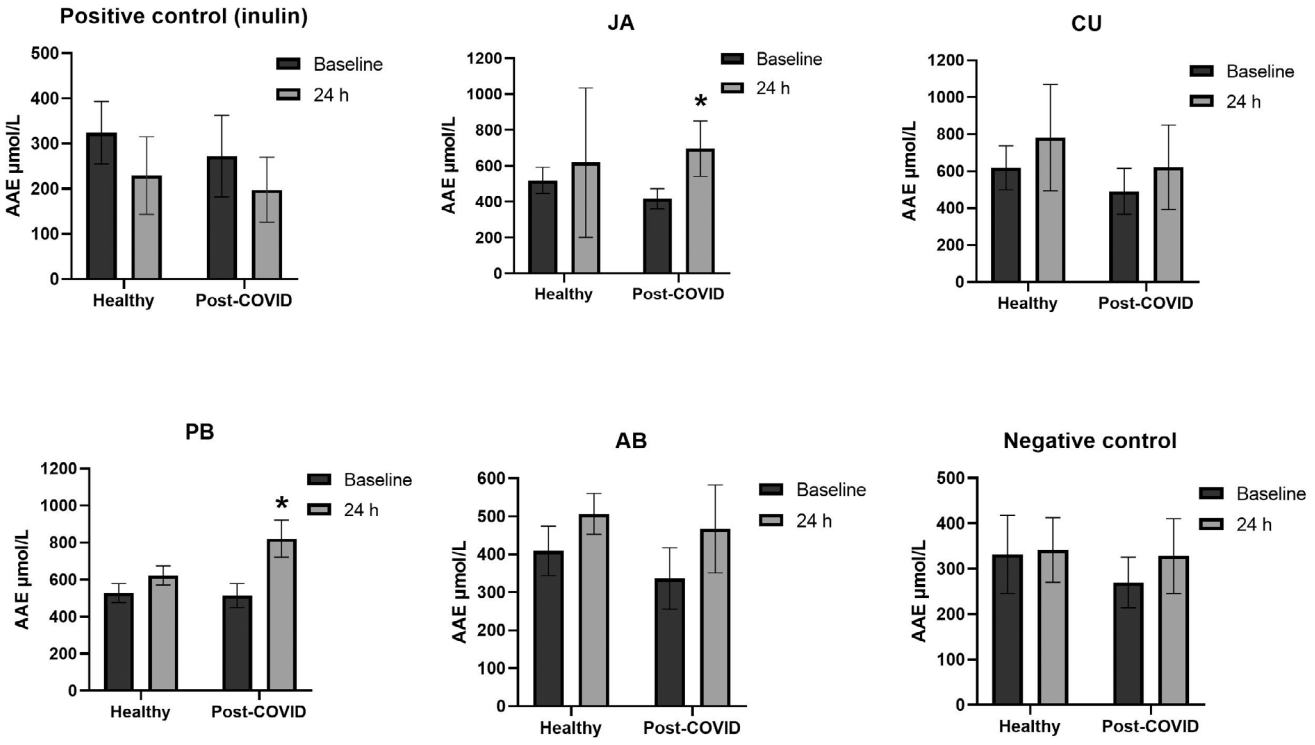

Figure 5 FRAP results (µM ascorbic acid equivalent – AAE) of the supernatants collected at baseline and after 24 h of in vitro colonic fermentation of Brazilian fruit flours, inulin and negative control with stool samples from healthy and post-COVID-19 donors. AAE, ascorbic acid equivalent; AB, bocaiúva almond flour; CU, cumbaru almond flour; JA, jatobá pulp flour; PB, bocaiuva pulp flour. *Statistical differences after 24 h in the same donor ($P < 0.05$).

which limits our considerations on the beneficial health effects of fruit flours.

As for stool donors, we chose subjects who had COVID-19 (PC) and healthy volunteers (HD). Indeed, it has recently been hypothesised that the gut microbiota plays a key role in the context of COVID-19 and also contributes to its long-term effects after viral clearance (Groves *et al.*, 2020; Lau *et al.*, 2022; Sun *et al.*, 2022). In particular, reduced bacterial diversity, together with a reduction in the relative abundance of health-associated bacteria such as SCFA producers belonging to the *Lachnospiraceae* and *Ruminococcaceae* families, has been observed in patients with COVID-19 (Gaibani *et al.*, 2021; Ren *et al.*, 2021; Yeoh *et al.*, 2021). In our dataset, although the reduction in biodiversity is consistent with what is commonly observed in *in vitro* models, it was possible to confirm the depletion of some taxa generally considered health-promoting in PC, such as *Ruminococcus*, *Christensenellaceae and Akkermansia* (Gu *et al.*, 2020; Tao *et al.*, 2020; Gaibani *et al.*, 2021; Lau *et al.*, 2022; Nashed *et al.*, 2022). We also confirmed PC-related enrichment in potential opportunistic pathogens, including *Veillonellaceae* members (Gu *et al.*, 2020; Tao *et al.*, 2020).

Taking into account the impact of fruit extracts on the faecal-derived microbial communities, it is interesting to note that the jatobá extract counteracted the increase of *Veillonellaceae* in PC while that of bocaiuva almond the further decrease of *Ruminococcus*. Moreover, the fermentation of the bocaiuva almond led to an enrichment of *Lactobacillus* and *Bifidobacterium*, underlining a relevant prebiotic potential.

TPC and FRAP analyses were conducted to analyse the content of total phenolic compounds and antioxidants during colonic fermentation, considering that gut bacteria may be involved in their biotransformation, as reported in some simulated *in vitro* models (Gibson *et al.*, 2017). However, it was not possible to observe differences in TPC between baseline and after 24 h, whereas in the FRAP analysis only for jatobá and bocaiuva pulp flours (PC donors), an increase in antioxidant activity was observed. It is estimated that 90%–95% of polyphenols contained in food are not absorbed by the small intestine and, therefore, can reach the colon (Gibson *et al.*, 2017). However, the amount of phenolic compounds and antioxidants that reach the colon and the bloodstream is limited compared to the content found in food right after consumption, as these

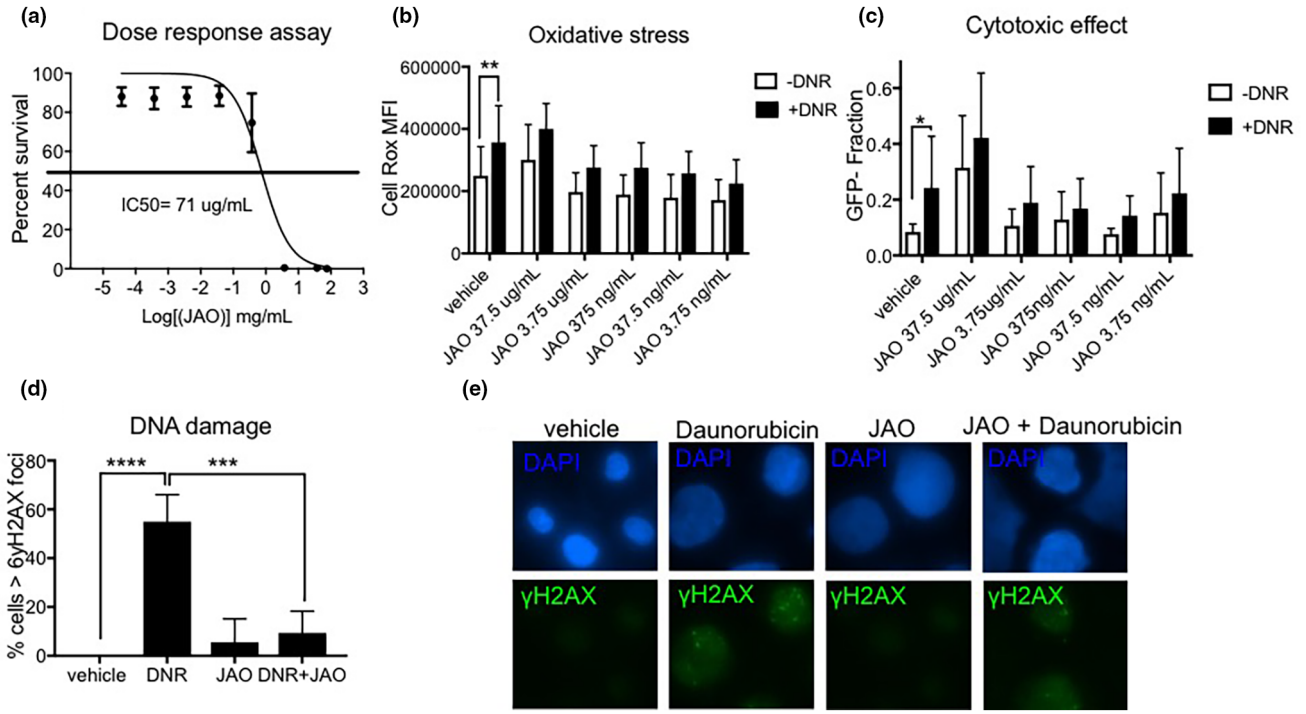

Figure 6 Effect of Jatobá pulp oil (JAO) on daunorubicin-induced oxidative stress and DNA damage. (a) IC50 of Jatobá pulp oil (JAO) in macrophage cell line MV411. Non-linear regression concentration/response curve reporting cell viability, determined by Trypan blue exclusion upon treatment with JAO for 72 h. Data are shown as average ± SD of triplicate wells and are representative of four independent experiments. The IC50 was calculated using GraphPad Prism software. (b) JAO protects from the oxidative stress induced by daunorubicin. The bar chart reports the oxidative stress as Median Fluorescence Intensity (MFI) of Cell ROX for MV411 pre-treated with either vehicle (DMSO) or increasing concentrations of JAO for 24 h before incubation with daunorubicin (DNR 25 nM) for additional 24 h. Data show mean ± SD of triplicate wells and are representative of four independent experiments. A 2-way ANOVA Sidak's multiple comparison test $^{**}P < 0.01$. (c) JAO protects from the cytotoxic effect of daunorubicin. The bar chart reports the cytotoxic effect as a fraction of GFP-cells for MV411 pre-treated with either vehicle (DMSO) or increasing concentrations of JAO for 24 h before incubation with 25 nM DNR for an additional 24 h. Data show mean ± SD of triplicate wells and are representative of four independent experiments. A 2-way ANOVA Sidak's multiple comparison tests $^{*}P < 0.05$. (d) JAO protects from the DNA damage induced by daunorubicin. The bar chart reports the DNA damage as a percentage of MV411 cells with more than 6 γH2AX foci. The cells were pre-treated with either vehicle (DMSO) or 37 ng/mL of JAO for 24 h before incubation with 25 nM DNR for an additional 48 h. Data show mean ± SD of triplicate wells and are representative of four independent experiments. A 2-way ANOVA Tukey's multiple comparison tests $^{***}P < 0.001$. $^{****}P < 0.0001$. (e) Digital microscope images showing DNA damage γH2AX foci in MV411 cells pre-treated with either vehicle (DMSO) or 37 ng/mL of JAO for 24 h before incubation with 25 nM DNR for an additional 4 h. Images were captured using Evos FL Digital Inverted Fluorescence Microscope (a particular from magnification 40×).

substances are highly reactive to alkaline conditions and can be easily oxidised, resulting in degradation or failure to detect (Lafarga *et al.*, 2019). Furthermore, the basal medium used in the colonic fermentation simulation contains microorganisms that degrade and convert components in the medium, such as phenolic compounds into phenolic acid or lactone metabolites (Aura & Maukonen, 2015). In juçara pulp, a fruit with a high content of phenolic compounds and anthocyanins, Guergoletto *et al.* (2016) found a decrease in the amount of these components after simulated digestion, indicating degradation by gut bacteria during the fermentation process.

Phenolic compounds have gained a lot of attention as a dietary intervention to augment endogenous oxidative defences. This is important because ROS can damage DNA, proteins and lipids and trigger pathogenetic processes. Most importantly, ROS are not only the result of exposure to genotoxic substances of environmental origin but also are continuously produced in aerobic organisms both as by-products of normal oxygen metabolism and as bactericidal agents by activated phagocytic cells. Therefore, a correct redox balance is considered very important for the prevention and treatment of various degenerative diseases, including cancer (Schieber & Chandel, 2014; Robinson *et al.*, 2021).

Finally, we chose to test the antioxidant properties of jatobá pulp in a cell model because JAO is known to contain bioactive substances such as g-tocopherol, b-sitosterol, campesterol, stigmasterol and stigmastanol (Oliveira *et al*., 2018), which could protect cells by hindering the harmful action of free radicals. Cell models are extremely useful and well-characterised experimental models that can be employed to investigate the effect of genetic and pharmacological manipulations, as well as the delicate balance between pro- and antioxidant activities. The oxidative response is particularly prevalent in cells of the innate immune system, including granulocytes, monocytes and macrophages, as it is central to the antimicrobial action of these cells. Therefore, myelo-monocytic cell lines such as MV411 and THP1 represent gold-standard experimental models for studying the mechanisms of redox homeostasis (Karwaciak *et al*., 2017).

After determining the IC50 of JAO in the myelomonocytic cell line MV411, we decided to further test non-toxic, nutritional concentrations (from 3.75 ng/mL to 37.5 μg/mL), which could be easily reached in the bloodstream and other tissues with an ordinary intake of fruits. In our study, JAO showed a protective antioxidant and antigenotoxic effect as it was able to reduce both oxidative stress and DNA damage induced by daunorubicin. Our data are in agreement with Spera *et al*. (2019) that showed that *H. courbaril* seed extract possessed antioxidant and antigenotoxic properties. However, the authors also reported that high concentrations of *H. courbaril* extracts (50–100 μg/mL) possessed a cytotoxic effect against B16F10 murine melanoma cells. More studies are therefore needed to evaluate the effects of non-nutritional concentrations of JAO in cancer cells and explore JAO as a pharmacological tool (Halliwell, 2013), as it has been reported for resveratrol and hydroxytyrosol, polyphenols abundant in edible plants such as grapes, olives and annurca apples (Corona *et al*., 2009; Borska *et al*., 2016; Martino *et al*., 2019).

Conclusions

To the best of our knowledge, this is the first *in vitro* study to evaluate the impact of native fruit flours from the Brazilian Cerrado and Pantanal on gut microbiota composition and metabolic profile. In addition to their high nutritional value, some of these fruit flours showed a promising ability to modulate gut microbiota imbalances, which could be relevant in post-COVID-19. We also showed that JAO has chemopreventive effects as it reduces daunorubicin-induced oxidative stress, DNA damage and cytotoxic effect. Taken together, these preliminary data demonstrate all the strengths and limitations of our study and lay the foundations for the design of an *in vivo* human intervention study to confirm the promising trends herein observed, along with studies in animal models to unravel the underlying mechanisms and evaluate the potential role of these flours in other contexts as well.

Acknowledgements

We would like to thank the Coordination for the Improvement of Higher Education Personnel (CAPES – Brazil), for the scholarship granted to C.S.I. Mauro (process number 88881.624468/2021-01), and the Department of Life Sciences at University of Roehampton (London, UK).

Author contributions

Carolina Saori Ishii Mauro: Conceptualization (equal); formal analysis (equal); investigation (equal); writing – original draft (equal). **Maryame Kadiri Hassani:** Formal analysis (equal); investigation (equal); writing – original draft (equal). **Monica Barone:** Formal analysis (equal); writing – review and editing (equal). **Maria Teresa Esposito:** Formal analysis (equal); writing – review and editing (equal). **Yolanda Calle:** Writing – review and editing (equal). **Volker Behrends:** Formal analysis (equal); writing – review and editing (equal). **Sandra Garcia:** Writing – review and editing (equal). **Patrizia Brigidi:** Writing – review and editing (equal). **Siliva Turroni:** Formal analysis (equal); writing – review and editing (equal). **Adele Costabile:** Conceptualization (equal); formal analysis (equal); writing – review and editing (equal).

Conflict of Interest

The authors declare no conflict of interests.

Ethical Guidelines

The University of Roehampton Research Ethics Committee (LSC 18-241) approved this study in accordance with the Declaration of Helsinki.

PEER REVIEW

The peer review history for this article is available at https://publons.com/publon/10.1111/ijfs.16274.

Data Availability Statement

Sequence reads were deposited in the National Center for Biotechnology Information Sequence Read Archive (NCBI SRA; BioProject ID PRJNA913064).

References

Al-Aamriri, H.M., Ku, H., Irving, H.R., Tucci, J., Meehan-Andrews, T. & Bradley, C. (2019). Time dependent response of daunorubicin on cytotoxicity, cell cycle and DNA repair in acute lymphoblastic leukaemia. *BMC Cancer*, **19**, 179.

Arruda, H.S., Araújo, M.V.L. & Marostica Junior, M.R. (2022). Underexploited Brazilian Cerrado fruits as sources of phenolic compounds for diseases management: a review. *Food Chemistry: Molecular Sciences*, **5**, 100148. https://doi.org/10.1016/j.fochms.2022.100148

This review stresses the relevance of phenolic-rich extracts from different parts of Brazilian Cerrado fruits for the treatment/management of various pathological conditions (e.g., cancer, diabetes, obesity, parasitic diseases, inflammation).

Aura, A.M. & Maukonen, J. (2015). One compartment fermentation model. In: *The Impact of Food Bioactives on Health*. Pp. 281–292. Cham: Springer. https://doi.org/10.1007/978-3-319-16104-4_25

Behrends, V., Tredwell, G.D. & Bundy, J.G. (2011). A software complement to AMDIS for processing GC-MS metabolomic data. *Analytical Biochemistry*, **415**(2), 206–208.

Benzie, I.F. & Strain, J.J. (1996). The ferric reducing ability of plasma (FRAP) as a measure of "antioxidant power": the FRAP assay. *Analytical Biochemistry*, **239**(1), 70–76.

Bezerra, G.P., da Silva Góis, R.W., de Brito, T.S. *et al.* (2013). Phytochemical study guided by the myorelaxant activity of the crude extract, fractions and constituent from stem bark of *Hymenaea courbaril* L. *Journal of Ethnopharmacology*, **149**, 62–69.

Bifari, F., Ruocco, C., Decimo, I., Fumagalli, G., Valerio, A. & Nisoli, E. (2017). Amino acid supplements and metabolic health: a potential interplay between intestinal microbiota and systems control. *Genes & Nutrition*, **12**, 27.

Bligh, E.G. & Dyer, W.J. (1959). A rapid method of total lipid extraction and purification. *Canadian Journal of Biochemistry and Physiology*, **37**(8), 911–917. https://doi.org/10.1139/o59-099

Bolyen, E., Rideout, J.R., Dillon, M.R. *et al.* (2019). Reproducible, interactive, scalable and extensible microbiome data science using QIIME 2. *Nature Biotechnology*, **37**, 852–857.

This article presents the QIIME 2 tool that has enabled great advances in microbiome research, enabling accessible, community-driven microbiome data science.

Borska, S., Pedziwiatr, M., Danielewicz, M. *et al.* (2016). Classical and atypical resistance of cancer cells as a target for resveratrol. *Oncology Reports*, **36**, 1562–1568.

Bortolotto, I.M., Hiane, P.A., Ishii, I.H. *et al.* (2017). A knowledge network to promote the use and valorization of wild food plants in the Pantanal and Cerrado. *Brazil. Regional Environmental Change*, **17**, 1329–1341.

Buford, T.W. (2017). (Dis)Trust your gut: the gut microbiome in age-related inflammation, health, and disease. *Microbiome*, **5**, 80.

Callahan, B.J., PJ, M.M., Rosen, M.J., Han, A.W., Johnson, A.J. & Holmes, S.P. (2016). DADA2: high-resolution sample inference from Illumina amplicon data. *Nature Methods*, **13**(7), 581–583.

Chhibber-Goel, J., Gopinathan, S. & Sharma, A. (2021). Interplay between severities of COVID-19 and the gut microbiome: implications of bacterial co-infections? *Gut Pathogens*, **13**(14), 2021.

Corona, G., Deiana, M., Incani, A., Vauzour, D., Dessì, M.A. & Spencer, J.P. (2009). Hydroxytyrosol inhibits the proliferation of human colon adenocarcinoma cells through inhibition of ERK1/2 and cyclin D1. *Molecular Nutrition & Food Research*, **53**, 897–903.

Corona, G., Kreimes, A., Barone, M. *et al.* (2020). Impact of lignans in oilseed mix on gut microbiome composition and enterolignan production in younger healthy and premenopausal women: an in vitro pilot study. *Microbial Cell Factories*, **19**, 1–14.

Costabile, A., Kolida, S., Klinder, A. *et al.* (2010). A double-blind, placebo-controlled, cross-over study to establish the bifidogenic effect of a very-long-chain inulin extracted from globe artichoke (*Cynara scolymus*) in healthy human subjects. *British Journal of Nutrition*, **104**, 1007–1017.

Culhane, A.C., Thioulouse, J., Perrière, G. & Higgins, D.G. (2005). MADE4: an R package for multivariate analysis of gene expression data. *Bioinformatics*, **21**(11), 2789–2790.

Damasceno-Junior, G.A. & de Souza P.R. (2010). *Sabores do Cerrado e Pantanal: conhecer para valorizar os frutos nativos; receitas e boas práticas de aproveitamento*. Pp. 142. Campo Grande, Brazil: Editora da Universidade Federal de Mato Grosso do Sul.

de Vos, W.M., Tilg, H., Van Hul, M. & Cani, P.D. (2022). Gut microbiome and health: mechanistic insights. *Gut*, **71**(5), 1020–1032.

Esposito, M.T., Zhao, L., Fung, T.K. *et al.* (2015). Synthetic lethal targeting of oncogenic transcription factors in acute leukemia by PARP inhibitors. *Nature Medicine*, **21**, 1481–1490.

Gaibani, P., D'Amico, F., Bartoletti, M. *et al.* (2021). The Gut Microbiota of Critically Ill Patients With COVID-19. *Frontiers in Cellular and Infection Microbiology*, 683–689. https://doi.org/10.3389/fcimb.2021.670424

In this article, the authors profiled intestinal dysbiosis in COVID-19 patients, showing a peculiar overrepresentation of Enterococcus, closely related to intensive care unit admission and the development of bloodstream infections.

Gibson, G.R., Hutkins, R., Sanders, M.E. *et al.* (2017). Expert consensus document: the International Scientific Association for Probiotics and Prebiotics (ISAPP) consensus statement on the definition and scope of prebiotics. *Nature Review Gastroenterology and Hepatology*, **14**(8), 491–502.

Groves, H.T., Higham, S.L., Moffatt, M.F., Cox, M.J. & Tregoning, J.S. (2020). Respiratory viral infection alters the gut microbiota by inducing inappetence. *mBio*, **11**, e03236-19.

Gu, S., Chen, Y., Wu, Z. *et al.* (2020). Alterations of the gut microbiota in patients with coronavirus disease 2019 or H1N1 influenza. *Clinical Infectious Diseases*, **71**(10), 2669–2678.

Guergoletto, K.B., Costabile, A., Flores, G., Garcia, S. & Gibson, G.R. (2016). *In vitro* fermentation of juçara pulp (*Euterpe edulis*) by human colonic microbiota. *Food Chemistry*, **196**, 251–258.

Halliwell, B. (2013). The antioxidant paradox: less paradoxical now? *British Journal of Clinical Pharmacology*, **75**(3), 637–644.

Hiane, P.A., Baldasso, P.A., Marangoni, S. & Macedo, M.L. (2006). Chemical and nutritional evaluation of kernels of bocaiuva, *Acrocomia aculeata* (Jacq.) Lodd. *Food Science and Technology*, **26**(3). https://doi.org/10.1590/S0101-20612006000300031

Jayaprakasam, B., Alexander-Lindo, R.L., DL, D.W. & Nair, M.G. (2007). Terpenoids from Stinking toe (*Hymneae courbaril*) fruits with cyclooxygenase and lipid peroxidation inhibitory activities. *Food Chemistry*, **105**(2), 485–490.

Joint WHO/FAO/UNU Expert Consultation (2007). *Protein and amino acid requirements in human nutrition*. Pp. 1–265, Vol. **935**. Geneva, Switzerland: World Health Organ technical report series.

Karwaciak, I., Gorzkiewicz, M., Bartosz, G. & Pulaski, L. (2017). TLR2 activation induces antioxidant defence in human monocyte-macrophage cell line models. *Oncotarget*, **8**(33), 54243–54264.

Keiji, T., Shimomura, K., Koizumi, Y., Mitsunaga, T. & Abe, I. (1999). Tyrosinase Inhibitors from the Pericarp of Jatoba (*Hymenaea courbaril* L.). *Natural Medicines*, **53**, 15–21.

Klindworth, A., Pruesse, E., Schweer, T. *et al.* (2013). Evaluation of general 16S ribosomal RNA gene PCR primers for classical and next-generation sequencing-based diversity studies. *Nucleic Acids Research*, **41**(1), e1.

Lafarga, T., Rodríguez-Roque, M.J., Bobo, G., Villaró, S. & Aguiló-Aguayo, I. (2019). Effect of ultrasound processing on the bioaccessibility of phenolic compounds and antioxidant capacity of selected vegetables. *Food Science and Biotechnology*, **28**, 1713–1721.

Lau, R.I., Zhang, F., Liu, Q., Su, Q., Chan, F.K. & Ng, S.C. (2022). Gut microbiota in COVID-19: key microbial changes, potential mechanisms and clinical applications. *Nature Reviews Gastroenterology & Hepatology*, 1–15. https://doi.org/10.1038/s41575-022-00698-4

Lee, S.C., Prosky, L. & Devries, J.W. (1992). Determination of total, soluble and insoluble dietary fiber in foods. Enzymatic-gravimetric method, MES-TRIS buffer: collaborative study. *Journal of the Association of the Official Analytical Chemists (AOAC) International*, **75**, 395–416.

Leeming, E.R., Louca, P., Gibson, R., Menni, C., Spector, T.D. & Le Roy, C.I. (2021). The complexities of the diet-microbiome relationship: advances and perspectives. *Genome Medicine*, **13**, 10.

Liu, Q., Mak, J.W., Su, Q. *et al.* (2022). Gut microbiota dynamics in a prospective cohort of patients with post-acute COVID-19 syndrome. *Gut*, **71**, 544–552.

Louis, P. & Flint, H.J. (2009). Diversity, metabolism and microbial ecology of butyrate-producing bacteria from the human large intestine. *FEMS Microbiology Letters*, **294**(1), 1–8.

Marrocco, F., Delli Carpini, M., Garofalo, S. *et al.* (2022). Short-chain fatty acids promote the effect of environmental signals on the gut microbiome and metabolome in mice. *Communication Biology*, **5**, 517.

Here, the authors explored the beneficial roles of SCFAs, particularly in influencing neuroimmune system and microglial activity, including learning and memory abilities, anxious behavior, neurogenesis, hippocampal plasticity and neurotrophin production.

Martino, E., Vuoso, D.C., D'Angelo, S. *et al.* (2019). Annurca apple polyphenol extract selectively kills MDA-MB-231 cells through ROS generation, sustained JNK activation and cell growth and survival inhibition. *Scientific Reports*, **9**, 13045.

Masella, A.P., Bartram, A.K., Truszkowski, J.M., Brown, D.G. & Neufeld, J.D. (2012). PANDAseq: paired-end assembler for Illumina sequences. *BMC Bioinformatics*, **13**, 31.

Merril, A.L. & Watt, K.B. (1973). *Energy Value of Foods: Basis and Derivation*. Washington: United States Department of Agriculture.

Nashed, L., Mani, J., Hazrati, S. *et al.* (2022). Gut microbiota changes are detected in asymptomatic very young children with SARS-CoV-2 infection. *Gut*, **71**(11), 2371–2373.

Oliveira, F.G.S., de Souza Araújo, C., Rolim, L.A., Barbosa-Filho, J.M. & da Silva Almeida, J.R. (2018). The genus Hymenaea: a chemical and pharmacological review. In: *Studies in Natural Products Chemistry* (edited by F.R.S. Atta-ur-Rahman). Pp. 339–388, Vol. **Chap. 12**. Amsterdam: Elsevier.

Pascale, A., Marchesi, N., Marelli, C. *et al.* (2018). Microbiota and metabolic diseases. *Endocrine*, **61**, 357–371.

Ren, Z., Wang, H., Cui, G. *et al.* (2021). Alterations in the human oral and gut microbiomes and lipidomics in COVID-19. *Gut*, **70**(7), 1253–1265.

Robinson, A.J., Davies, S., Darley, R.L. & Tonks, A. (2021). Reactive oxygen species rewires metabolic activity in acute myeloid leukemia. *Frontiers in Oncology*, **11**, 632623.

Rognes, T., Flouri, T., Nichols, B., Quince, C. & Mahé, F. (2016). VSEARCH: a versatile open source tool for metagenomics. *PeerJ*, **4**, e2584.

Schieber, M. & Chandel, N.S. (2014). ROS function in redox signaling and oxidative stress. *Current Biology*, **24**(10), R453–R462.

Silva, Y.P., Bernardi, A. & Frozza, R.L. (2020). The role of short-chain fatty acids from gut microbiota in gut-brain communication. *Frontiers in Endocrinology*, **11**, 25.

Song, H.E., Lee, H.Y., Kim, S.J., Back, S.H. & Yoo, H.J. (2019). A facile profiling method of short chain fatty acids using liquid chromatography-mass spectrometry. *Metabolites*, **9**, 173.

Spera, K.D., Figueiredo, P.A., Santos, P.C. *et al.* (2019). Genotoxicity, anti-melanoma and antioxidant activities of *Hymenaea courbaril* L. seed extract. *Annals of the Brazilian Academy of Sciences*, **91**, e20180446.

Sun, Z., Song, Z.G., Liu, C. *et al.* (2022). Gut microbiome alterations and gut barrier dysfunction are associated with host immune homeostasis in COVID-19 patients. *BMC Medicine*, **20**, 24.

Swain, T. & Hills, W.E. (1959). The phenolic constituents of *Prunus domestica*. *Journal of the Science of Food and Agriculture*, **10**, 63–69.

Tao, W., Zhang, G., Wang, X. *et al.* (2020). Analysis of the intestinal microbiota in COVID-19 patients and its correlation with the inflammatory factor IL-18. *Medicine in Microecology*, **5**, 100023.

Wilmes, P., Martin-Gallausiaux, C., Ostaszewski, M. *et al.* (2022). The gut microbiome molecular complex in human health and disease. *Cell Host and Microbe*, **30**(9), 1201–1206.

Yeoh, K.Y., Zuo, T., Lui, G.C. *et al.* (2021). Gut microbiota composition reflects disease severity and dysfunctional immune responses in patients with COVID-19. *Gut*, **70**(4), 698–706.

Supporting Information

Additional Supporting Information may be found in the online version of this article:

Figure S1. The alpha diversity of faecal-derived microbial communities from post-COVID-19 and healthy donors tends to decrease over time in 24-h fermentation experiments in the presence of fruit flours, inulin or without additions. Boxplots showing the distribution of alpha diversity values, according to the Shannon index (upper panel) and the number of observed amplicon sequence variants (ASVs, lower panel), for the faecal-derived microbial communities from post-COVID-19 (PC) and healthy (HD) donors at time point 0, 4, 6 and 24 h of fermentation (T0, T4, T6 and T24) in the presence of fruits flours (jatobá, cumbaru, bocaiuva pulp and bocaiuva almond), inulin or without additions (control -).

Figure S2. Unweighted UniFrac-based principal coordinates analysis (PCoA) of faecal-derived microbial communities of post-COVID-19 and healthy donors over 24 h of fermentation in the presence of fruit flours, inulin or without additions. Left, PCoA plot showing all fermentation samples, coloured by a group of donors (post-COVID-19 donors, PC, red vs. healthy donors, HD, blue). A significant separation between groups was found, regardless of experimental condition (fruit flours, inulin and negative control) and time point (0, 4, 6 and 24 h of fermentation – T0, T4, T6 and T24) ($P < 0.001$, PERMANOVA). Right, PCoA plots show the fermentation samples for PC (top panel) and HD (bottom panel). Within each group of donors, the samples were separated significantly by experimental condition (fruit flours, inulin and negative control) and time point (T0, T4, T6 and T24) ($P < 0.001$).

Figure S3. Effect of Jatobá pulp oil (JAO) alone or in combination with daunorubin on oxidative stress and viability. MV411 cells were infected with a lentiviral vector expressing eGFP and positive cells were isolated by cell sorting. The GFP fluorescence emission is proportional to the number of cells. Representative FACS plots indicating the Forward and Side scatter of MV411 cells included in the analysis (population P1),

the gating strategy to exclude duplets from the analysis (population P2), the gates M1 and M2 to discriminate GFP− from GFP+ cells and the gate M7 that reports the intensity of oxidative stress.

Figure S4. Effect of Jatobá pulp oil (JAO) alone or in combination with daunorubin on DNA damage. Digital microscope images showing DNA damage γH2AX foci in MV411 cells pre-treated with either vehicle (DMSO) or 37 ng/mL of JAO for 24 h before incubation with 25 nM DNR for an additional 48 h. Images were captured using Evos FL Digital Inverted Fluorescence Microscope (magnification 40×).